Available online at https://sej.journals.ekb.eg/
FACULTY OF ENGINEERING – SOHAG UNIVERSITY
Sohag Engineering Journal (SEJ) Vol. 3, No. 1, March 2023

Performance Enhancement of PMSG by Optimal Control Strategy and Crowbar Protection Using Novel Optimization Algorithm

Abd-Elhady Ramadan[a], Khairy Sayed [a], Mohamed Ebeed [a,b] * Salah Kamel[c], Ahmed Refai[a], Francisco Jurado[b]

[a] *Electrical Engineering Department, Sohag University, 82524, Sohag, Egypt*
[b] *Department of Electrical Engineering, University of Jaén, 23700 EPS Linares, Jaén, Spain.*
[c] *Electrical Engineering Department, Faculty of Engineering, Aswan University, Aswan 81542, Egypt.*

Abstract

Renewable energy resources (RERs) are widely embedded in the power system due to the fossil fuel depletion, economic and environmental issues. The permanent magnet synchronous generator (PMSG) is considered one of the most promising technologies for the wind energy conversion system (WECS). However, in case of faults occurrence the behavior of the PMSG will be changed considerably. The crowbar protection is the most common used for reduce the negative effects of the faults. The resistors of the crowbar should be determined preciously to ensure the best performance of the WECS based PMSG based during the system faults. The aim of this paper is to investigate the performance of the WECS based PMSG under grid faults with optimal integration of the Crowbar protection system. The Lightning Attachment Procedure Optimization (LAPO) is employed to find the optimal values of the crowbar's resistors to mitigate the fault effects. The simulation results reveal to that the performance of the WECS based PMSG can be enhanced considerably with optimal inclusion of the crowbar protection in terms of the stator current, the DC voltage, the delivered active and reactive powers to the grid under faults of states.

 DOI: 10.21608/SEJ.2022.160011.1021

Keywords:wind turbines; PMSG;WECS; crobar protection system; grid faults; LAPO optimizer

1. INTRODUCTION

Renewable energy sources are very important as they provide clean and cheap power with respect to the traditional energy sources based on fossil fuels[1, 2]. During the previous few years, using the renewable energy sources like solar, wind, hydro, and tidal based sources grow very fast. For renewable energy resources (RERs), there are many advantages where RERs are considered clean energy sources, because these resources don't inject any harmful gases in the atmosphere. Wind energy is considered among the most attractive, vital and efficient types of renewable energy sources. Producing the electricity from wind farms is very important because it is a clean and has low cost compared with the other types of renewable energy resources[1, 3].

There are many improvements have been applied in the wind energy conversion system (WECS) in order to handle with the fast growth in the new technology of wind conversion system. The wind turbine (WT) is the most important part of WECS as it can produce a mechanical power from the incident wind kinetic energy[4, 5]. There are two types of wind turbine configurations which have been used in the wind energy conversion systems. The first type is the fixed speed wind turbine (FSWT) which is distinguished with that its construction is simple and its wind speed range is narrow. The second type is the variable speed wind turbine (VSWT) which is most commonly used compared with (FSWT). The VSWT has many advantages including high extracted wind energy, low mechanical stress, as well as its speed range is wide which is completely controlled[3, 6]

There are number of different types of generators are used in variable speed WECSs such as the doubly fed induction generators (DFIGs), the squirrel cage induction generators (SCIGs) and the permanent magnet synchronous generators (PMSGs) [7]. It should be highlighted here that using the PMSGs can enhance the performance of the WECS by 10% [9,10]. PMSGs are connected to the national grid through power converters[8, 9] . The WECS based on the PMSG includes an AC-DC-AC power converter, which consists of three main parts

* Corresponding author: author@institute.xxx .

including wo converters and a DC bus, as shown in Fig.1.[1], the first converter is the machine side converter (MSC) and the other one is the grid side converter (GSC). The machine side converter (MSC) is applied for extracting the maximum generated power from the PMSG, in the other hand the grid side converter (GSC) is used for supplying only the active power to the national grid and mitigate the reactive power [10]. As well as the grid side converter (GSC) is employed to regulate the supplied voltage and frequency to the power grid and used to achieve the stability of the grid during faults or abnormal operation conditions[6]. The most common controllers for the control system of the MSC and GSC are the proportional integral (PI) controllers[11], the fuzzy logic controllers (FLCs) [12], and the slide mode controllers. The PI controllers are still commonly applied in the many controls system specially the wind energy system this is due to their fast response and ease of parameter settings. However, these controllers have negative effects with the nonlinear system changes and variations. Therefore, the metaheuristic algorithms and optimization techniques are applied for determining the optimal values of the PI controllers parameter setting [3]. The wind energy conversion system can subject several abnormal conditions such as three phase symmetrical and unsymmetrical faults, lightening and flicker, etc. [13]. These faults have negative effects on the WECS including the three-phase short circuit fault leads to voltage dips and high currents in the stator windings of the PMSG as well as in the DC–link voltage of the converters. These currents may cause damage the converters of the WECS based on PMSG. Therefore, it is mandatory provide a robust protection for the WECS socially the PMSG,DC bus capacitor and converters to avoid the dangerous effects [14, 15]. The crowbar protection system is an efficient protection system which has been applied to protect the WECS based on PMSG components in case of faults occurrence [16]. It should be highlighted here that after fault clearance the crowbar protection will be deactivated after a certain controlled time. The crowbar protections affects the dynamic response and behavior of the PMSG during and after fault clearance [14, 17]. There are many types of the crowbar protection systems, the crowbar protection systems are classified based on their construction and operation methodology including the passive crowbar protection, the active crowbar protection, the series crowbar protection and the outer crowbar protection [15, 18].

This paper depicts the performance of the WECS based on PMSG under three phase to ground fault and how to mitigate the dangerous effects of this type of faults using an outer crowbar protection system. It should be highlighted here that the LAPO optimizer is used to determine the optimal value of the crowbar protection current limiter resistors. The rest of paper is organized as follows: Section 2 shows the modeling of the WECS based on PMSG and the discretion of the crowbar protection systems. Section 3 gives an overview about the LAPO algorithm. Section 4 describe the used objective function. Section 5 lists the simulation results along with the discussion. Finally, the conclusion of this paper is listed section 6.

2. MODELING OF THE WECS BASED ON THE PMSG

The wind energy conversion system is used for converting and supplying the electric power to the electrical national grid. The WECS based PMSG consists of the variable speed wind turbine, the PMSG, the MSC, the GSC and the DC bus capacitor as shown in Fig. 1. The wind turbine which connected directly to the PMSG is used for extracting mechanical power from the kinetic energy of the incident wind, the PMSG converts the wind turbine mechanical power into electrical power. The fully controlled MSC is used to converts the generator AC power output into DC power to collect the maximum power of the PMSG in the case of wind speed changes while the fully controlled GSC is used to converts the DC power to an AC power to supply the national grid with active power at unity power factor using inductive filter (L_f), and a step-up power transformer through translation lines [19].

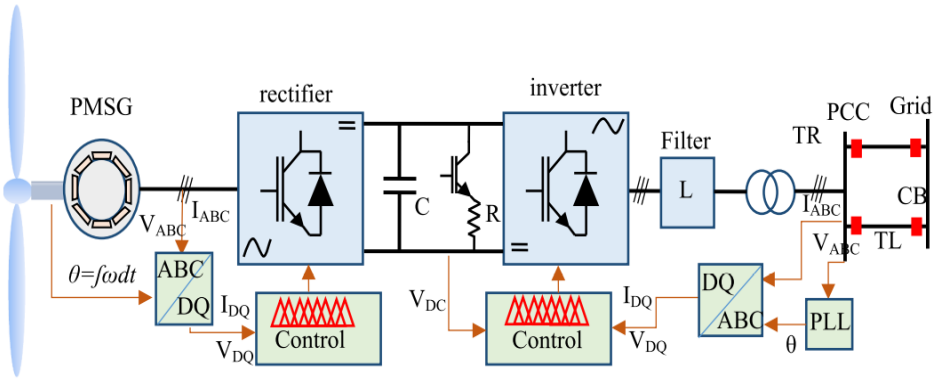

Fig. 1. Typical WECS based ON PMSG.

1.1. Wind turbine model

The horizontal-axis wind turbines with three-blades are the commonly used in the WECS. In these types, the generators are lied in the top of the turbine tower[6]. The captured power by the wind turbine and the mechanical torque developed are calculated using the following equations. The mechanical power included in the incident wind P_w can be calculated as in (1). The aerodynamic performance of the wind turbine is expressed as a function of the power coefficient $C_p(\lambda, \beta)$, which determines the ratio between the total power extracted by the wind turbine P_m and the incident wind power P_w as in (2). The power coefficient of the wind turbine depends on two parameters including the wind turbine blades pitch angleβ and the tip speed ratio λ , as in (3) the tip speed ratio is determined as in (5).

$$P_w = 0.5\rho_{air} A_b V_w^3 \tag{1}$$

$$Cp = \frac{P_m}{P_w} \tag{2}$$

$$C_p(\lambda, \beta) = 0.5176(116\gamma - 0.4\beta - 5)e^{-2\gamma t} + 0.0068\lambda \tag{3}$$

where γ is calculated as fallows.

$$\gamma = \frac{1}{\lambda + 0.8\beta} - \frac{0.035}{1 + \beta^3} \tag{4}$$

$$\lambda = \frac{\omega_m * R}{V_m} \tag{5}$$

$$P_m = T_m \omega_m \tag{6}$$

where P_w donates the incident wind kinetic power. P_m donates the mechanical power extracted by the wind turbine. ρ_{air} donates the density of the air which equals to 1.225 kg/m3. V_w represents the velocity of the incident wind. C_p represents Betz constant which equals to 0.593 [4]. A_b donates the turbine blades swept area T_m refers to the rotating mechanical torque that is produced by the turbine. ω_m donates the mechanical speed of the turbine rotor. R donates the radius of the blades. λ represents the tip speed ratio that is the ratio of the turbine rotor speed and the wind speed. β refers to the pitch angle of the wind turbine blades. Fig. 2 shows the relationship between the tip speed ratio and the power coefficient. The output mechanical power of WT is expressed in (2). Fig. 3 shows variations of the mechanical output power of the wind turbine against the rotor speed. From the previous equations, the mechanical output power of the wind turbine can be calculated as follows [6, 20]:

$$P_m = 0.5\rho_{air} A_b V_w^3 C_p \tag{7}$$

where $P_{w\,\max}$ donates the maximum extracted power which is calculated as in (8), where the optimal position of the maximum power is accomplished at $C_{p\,\max}$ = 0.48 and $\lambda_{\max}$ = 8.1, as shown in Fig. 2 [19].

$$P_{w\,\max} = 0.5\rho_{air} A_b C_{p\,\max} \left(\frac{\omega_m \times R}{V_m}\right)^3 \tag{8}$$

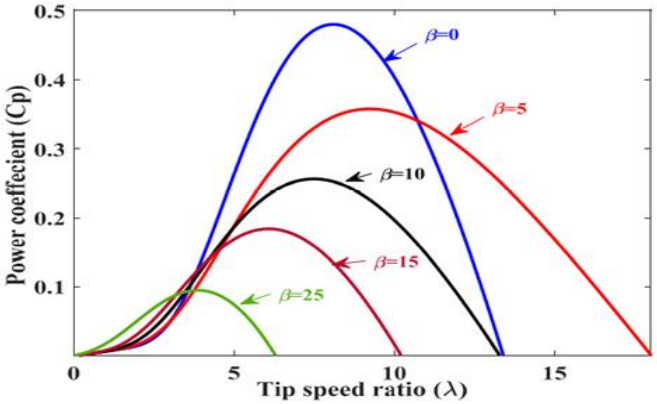

Fig. 2. The Cp typical characteristics.

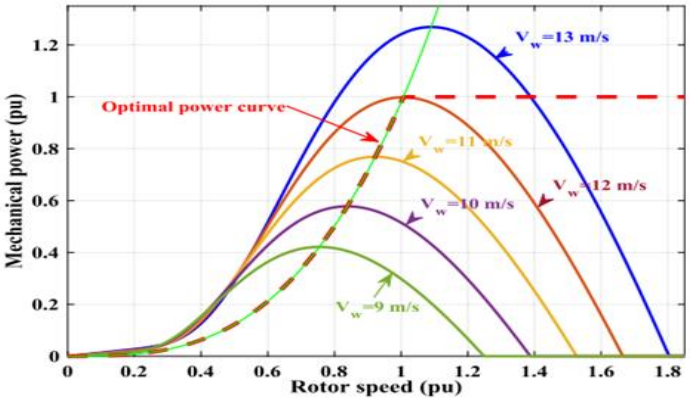

Fig. 3. VSWT output mechanical power characteristics.

1.2. PMSG gearless Shaft Modelling

The shaft of the PMSG rotor is connected directly to the of the wind turbine shaft without using any gearbox, which is known as direct-drive (DD) train. As a result, the PMSG shaft runs very slow, and the generated power has low frequency. Therefore, a frequency converter used to increase the frequency in the grid side (GSC). Due to that mechanical stresses of the PMSG shaft is small because of the using of the frequency converter which transfers the generated power from the gearless PMSG to the electrical national grid trough the DC bus capacitor. The DD train is considered as a single-mass shaft model. The of the single-mass shaft modeling is determined by (9) as follows:

$$-j\frac{d\omega_m}{dt} + D\omega_m = T_m - T_e \tag{9}$$

where D donates the rotor damping coefficient, j donates the rotor inertia, and T_e donates the developed electrical torque of the PMSG and T_m is the mechanical torque developed by the turbine [21].

1.3. PMSG-Side Modelling

The generator is used for converting the rotational mechanical power into electrical power, where the speed of the wind turbine rotor (ω_m) is considered as the input signal to the generator model, and its output signals are the stator voltages. The direct and quadrature axis voltages (V_d, V_q) of the PMSG stator are expressed as in (10).

$$\begin{bmatrix} V_d \\ V_q \end{bmatrix} = R_s \begin{bmatrix} I_d \\ I_q \end{bmatrix} - \frac{d}{dt}\begin{bmatrix} L_d I_d \\ L_q I_q \end{bmatrix} + \omega_g \begin{bmatrix} L_q I_q \\ -L_d I_d + \psi_f \end{bmatrix} \tag{10}$$

where R_s donates the resistance of the PMSG stator, ω_g donates the speed of the PMSG shaft and the ψ_f donates the flux of the rotor linked with the PMSG stator ,(I_d, I_q) represent the direct and quadrature axis

currents respectively and the inductances (L_d, L_q) represent the direct and quadrature axis inductances respectively [21].

For maximizing the power extracted from the incident wind by the WECS the MSC scheme is used. The field-oriented control (FOC) is used with the MSC to maximize wind power transferred from the PMSG. The field-oriented control (FOC) is employed in the MSC using two control loops including the outer control loop which is used to set the speed of the generator shaft to the optimal value using a suitable controller and the inner control loop which is applied for regulating the currents of the generator and generating the pulses used for switching the MSC[4].

1.4. Grid Side Modeling

The GSC is applied for transmitting the WECS generated power from MSC and the DC bus to the national grid, as shown in Fig. 1. Where The DC bus voltage is regulated using the voltage-oriented control (VOC) technique, where only the active power is transferred to the national grid. The voltage-oriented control (VOC) operates based on dual control loops, the first one is the DC bus voltage control loop which is applied to regulate the voltage of the DC bus capacitor in case of the variations occur in the generated power, the second one is the grid current control loop which used for mitigating the reactive power transferring to the national grid through reducing the component of the q-axis current of the grid to zero[4].

The power of the grid can be represented with an inductance connected in series with a controlled voltage source. Since the grid considered a very large capacity power system. The filter is represented by the total equivalent inductance (L_g), the transformer, and the double line transition line. The grid side converter terminal voltages (V_{id}, V_{iq}) are calculated as a function of the values of the grid currents (I_{gd}, I_{gq}) and the grid voltages (V_{gd}, V_{gq}) which are measured with respect to the common coupling point (PCC), as expressed in (10) [22].

$$\begin{bmatrix} V_{id} \\ V_{iq} \end{bmatrix} = \begin{bmatrix} V_{gd} \\ V_{gq} \end{bmatrix} + L_g \frac{d}{dt} \begin{bmatrix} I_{gd} \\ I_{gq} \end{bmatrix} \tag{11}$$

1.5. The Crowbar protection system

Recently the rapid increase of the capacity of installed wind farms in transmission systems makes it necessary that the WECS remains operating during power network disturbances[18]. Therefore, the recent codes of grid require that the wand farms must withstand a certain percentage of voltage dips with respect to the nominal voltage and for a certain time which known as Fault Ride Through (FRT) [18]. In the case of grid fault occurrence that would cause voltage dips, stator windings of the PMSG would induce high currents and the DC bus voltage would be very high which can damage the converter. For these reasons the crowbar protection is applied for protecting the WECS based on PMSG. After a certain time of grid fault occurrence, the crowbar protection system is activated this time depend on the response speed of the protection devices. After the clearance of the fault the crowbar protection system will be deactivated. There are different types of the crowbar protection systems depend on their construction and operation. These types of crowbar protection including the series crowbar protection which consists of three resistors in [15, 18]. parallel with a bidirectional static switch, the series crowbar is connected in series with the stator windings of the PMSG, the crowbar switch is switched on during the normal operation ,when the short circuit fault occurs the switch will be switched on, in this case the crowbar resistor will be in series with the stator windings and the high stator currents will pass through the resistors which used to limit these currents [15, 18]. The outer crowbar protection has the same construction of the series crowbar protection as it consists of three resistors in parallel with a bidirectional static switch and has almost the same operation of the series crowbar, but the outer crowbar connected in series with the PMSG instead of connecting in series with the stator windings, during the normal operation the outer crowbar switch is turned on, in the case of the short circuit fault occurrence the switch will be turned on, here the outer crowbar resistor will be in series with the PMSG and the high induced currents will pass through the resistors [18, 23]. The DC crowbar protection consists of a resistor in series with an IGBT switch. The DC Crowbar protection system is connected in parallel with the DC bus capacitor to protect the DC bus and the converter from the high rise of DC voltage due to faults. When a fault occurs, the excess active power will be dissipated in the DC crowbar resistor. Therefore, the DC crowbar protection is used to regulate the voltage of DC bus and reduce the overcharge due to the occurrence of fault. The switching control signal for the DC crowbar protection is automatically switched on/off whenever the DC-link voltage rises over/under its threshold value [18, 23].

3. LIGHTNING ATTACHMENT PROCEDURE OPTIMIZATION (LAPO)

Lightning Attachment Procedure Optimization (LAPO) is one of the novel optimization techniques planned and developed by A.F. Nematollahi et al. [24, 25]. LAPO optimizer simulates a natural phenomenon of the

Lightning. LAPO optimization technique involves five steps which are the initial spots, leader upward direction, section fading, downward leader one or orientation and the strike point which impressionists the optimal solution. LAPO has many advantages including high searching capability which help to apply LAPO for solving a lot of the optimization problems. In [26], There are many application where LAPO optimizer is applied including the using of LAPO to determine the optimal siting and sizing of controller of the unified power flow in transmission system, the optimal power flow solution in the power networks [27], LAPO optimization technique is used widely for find the optimal location and size of the distributed generators in the distribution networks.as well as LAPO is applied for Image Segmentation optimization[28]. LAPO working principle is explained as that before lightening occurrence there will be huge amounts of negative charges which lie on the upper part of the cloud, at the same time there will be a very large number of positive charges lie on the lower part of the cloud. The increasing of the negative charges occur rapidly as shown in Fig. (4). [29, 30]. A very high potential appears which in its turn causes the starting of breakdown between the negative charges in the upper part and the positive charges in the lower part of the cloud. The negative charge appears and increase very fast as a result the potential gradient between the cloud lower edge and the surface of the ground rises. The lightening will occur due to the fast rising of the potential gradient between the cloud lower edge and the ground surface. It should be highlighted here that the motion of the downward ladders of lightening are gradual and occurs in many directions[31].

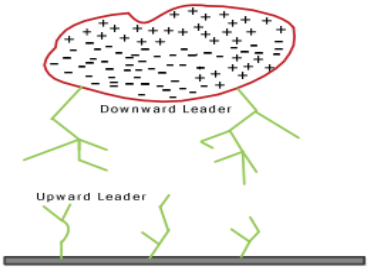

Fig. 4. The cloud charging form.

The Mathematical expression of LAPO algorithm including the following steps:

Step (1) Initialization

The initial test points which refer to the upward leaders starting points are represented by the initial search agents. It should be highlighted here that the upward leaders starting points are generated in a random way which can be found as follows:

$$A_s^i = A_{\min}^i + (A_{\max}^i - A_{\min}^i) * rand \quad (12)$$

where A_s^i denotes the initial test points,$A_{\min}^i$ and $A_{\max}^i$ denote the minimum and maximum limits of the control variables respectively, and $rand$ is a random value in the range of [0,1]. The objective function of the initial starting points can be founded as follows [29]:

$$F_s^i = \text{Objective } (A_s^i) \quad (13)$$

Step (2) Determination of the next jump

All downward leader average points are allocated as in (14), and the corresponding objective function is determined as in (15).

$$A_{avr} = \text{mean } (A_s) \quad (14)$$

$$F_{avr} = \text{Objective } (A_{\text{avr}}) \quad (15)$$

where A_{avr}donates downward leader average point, F_{avr} is the objective function of the downward leader average point. For updating the location of point i, another random point j is selected where i≠j. Then the determined point is compared with the point selected randomly. Hence, the next jump is found as in (16,17) [29, 30].

when $F(A_s^J) < F_{avr}$

$$A_{s\_\text{new}}^i = A_s^i + \text{rand} * (A_{\text{avr}} + A_s^i) \quad (16)$$

when $F(A_s^J) > F_{avr}$

$$A_{s\_\text{new}}^i = A_s^i - \text{rand} * (A_{\text{avr}} + A_s^i) \quad (17)$$

Step (3) Branch vanishes

The branch vanishes is achieved through the acceptance of anew point, this new point determines whether the branch vanishes are accepted or not by comparing the objective function value of the new point and the original point, as if the objective function of the new obtained is better than that of the original point then the new point is accepted as in (18,19). The branch vanishes step is applied on all points and all down ladder test points [31]:

$$A_s^i = A_{s\_new}^i \qquad IF \ F_{s\_\text{new}} < F_s^i \quad (18)$$

$$A^i_{s\_new} = A^i_s \qquad \text{Otherwise} \tag{19}$$

Step (4) upward Leader movement

This step shows the motion of the upward leader where all points here consider upward and travel upward. The upward leaders oriented in the same way of the downward leaders' motion. Where an exponential operator is used to control the downward leaders motion through the channel, which is expressed in (20) [31].

$$A^i_{s\_new} = A^i_{s\_new} + \text{rand} * S * (A^i_{best} - A^i_{worst}) \tag{20}$$

where S is expressed as follows

$$S = 1 - \left(\frac{T}{T_{max}}\right) \times e^{\left(\frac{T}{T_{max}}\right)} \tag{21}$$

where T and T_{max} represent the current iteration number, and the maximum number of iterations respectably, $\boldsymbol{A^i_{best}}$ donates the best solution while $\boldsymbol{A^i_{worst}}$ donates the worst solution within the populations [31].

Step (5) Strike point

This describe the final stage of lightening occurrence When the combination between the down leader and the up leader occurs. The lightning will paused through a certain point which is called the striking point [29].

The considered objective function.

4. OBJECTIVE FUNCTION

The considered objective function is the sum of the integral function of the DC bus voltage, the active power, the reactive power the stator side current, the stator side voltage, the grid side current and the grid side voltage squared errors. LAPO optimizer has been used to design the optimal values of the crowbar projection system resistor by the execution of the WECS based on PMSG model using MATLAB SIMULINK software. The model simulation time is 4 sec where the three phase to ground fault occurs at t=3 sec and the fault duration is 150 m sec. In this paper LAPO optimizer has been used to minimize the value of the objective function.

$$OF(x) = \int_0^4 \Big[(V^*_{DC} - V_{DC})^2 + \left(P_{max} - P_g\right)^2 + \left(Q_{ref} - Q_g\right)^2 + \left(V^*_{abc\_stator} - V_{abc\_stator}\right)^2 + \left(I^*_{abc\_stator} - I_{abc\_stator}\right)^2 + \left(V^*_{abc\_grid} - V_{abc\_grid}\right)^2 + \left(I^*_{abc\_grid} - I_{abc\_grid}\right)^2\Big] dt \tag{22}$$

where V_{DC} is the voltage of the DC bus, P_{max} and P_g represent the maximum and generated active power respectively, Q_{ref} and Q_g represent the reference and generated reactive power respectably, I_{abc_stator} is the stator currents in the machine side, V_{abc_stator}) is the stator voltages in the machine side, I_{abc_Grid} is the grid side currents and V_{abc_Grid} s the grid side voltages and x represents the optimal value of the crowbar protection system resistors(r) where $0.21 \le r \le 0.31$.

5. THE SIMULATION RESULTS

In this section, the performance of the wind energy conversion system based on PMSG is studied under three phase to ground grid fault and with optimal integration of the outer crowbar protection system type to deduce the dangerous effects of grid faults. The studied wind energy conversion system based on PMSG system is shown in Fig. 5. A three-phase fault to ground is occurred for 150 m Sec. As the simulating running time is 4 sec and the fault occur after 3 sec and continue for 150 m sec. Then, the fault is cleared. The parameters of the LAPO algorithm including the maximum number of iterations and number populations are selected to be 150 and 15, respectively. The program was conducted using MATLAB SIMULINK software (MATLAB 2015) and the simulation MATLAB system using is shown in Fig. 6. The system data are listed in Appendix A. The resistor optimal value equals 0.25867 ohm for each resistor of the crowbar protection system.

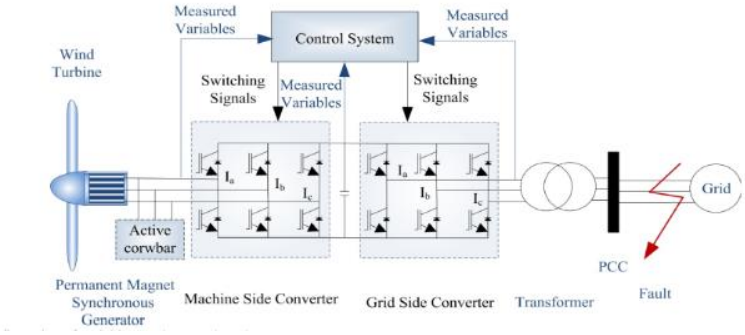

Fig. 5. Configuration of variable speed WECS based PMSG with grid fault.

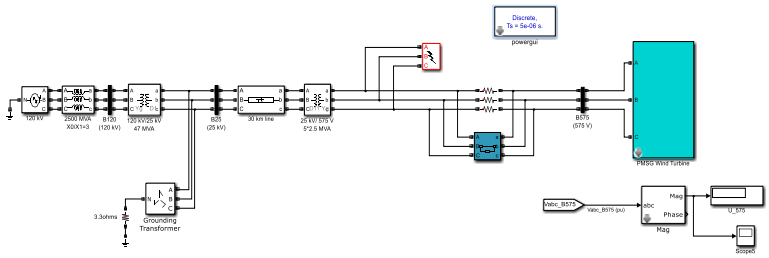

Fig. 6. The MATLAB SIMULINK model.

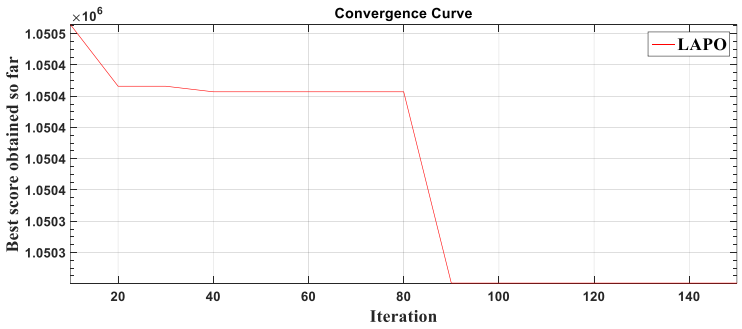

Fig. 7. Convergence of best values of norm function.

During the three-phase fault occurrence the DC link voltage increases because of the excessive power in the DC link, so an adverse overvoltage appears across the DC capacitors and can be damaged. These capacitors are protected using converter circuits. Fig.8. shows that the DC bus voltage raises during fault without using the crowbar protection system. While wit the using of the crowbar protection with optimal limiter resistor the DC bus voltage equals to its nominal values during fault. The active power during the fault and without the crowbar protection fails to zero. This means that the WECS based on PMSG does not supply power to the grid. While using the crowbar protection make the power in its nominal value (1 p.u.) which helping in the continuity of suppling the power to grid in case of grid fault occurrence as shown in Fig.9.

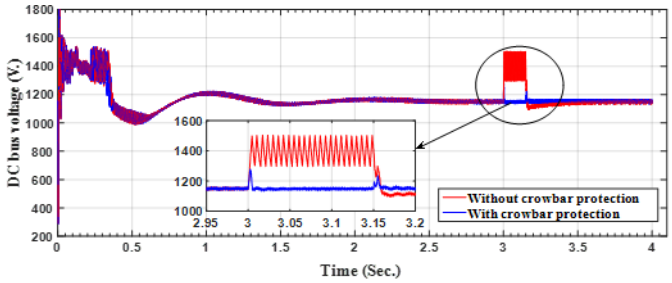

Fig. 8 The DC bus voltage with and without crowbar protection.

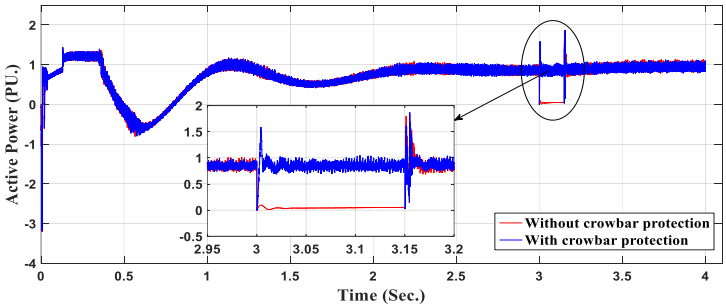

Fig. 9. The Active Power with and without crowbar protection.

PMSG based on WEC Supply the grid with apparent power with unity power factor which mean that there is no reactive power supplied to the grid and active power only is supplied. Fig. 10. shows that the reactive power is equal to zero during the normal operation. While during the fault the reactive power is negative which make

the WECS consume reactive power from the grid. In the case of fault, the using of protection crowbar helping to improve the reactive power profile during the fault occurrence.

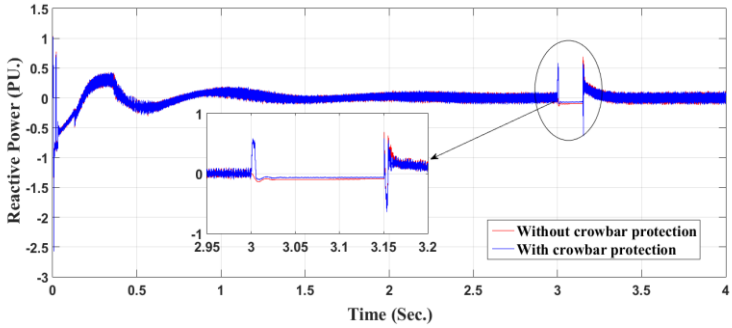

Fig. 10. The Reactive Power with and without crowbar protection.

The effect of the three phase to ground grid fault on the grid side current is shown in Fig.11. (a). As the grid current increase during the fault. Fig.11. (b). shows how the crowbar protection system is efficient in reducing the grid current to its nominal value during the fault duration.

Also, the grid fault affects the grid side voltage badly. As the grid voltage decrease and it almost reduces to zero during the fault as shown in Fig.12. (a). While with the use of crowbar protection system the grid side voltage came back to 1 PU (its nominal value I during the fault as shown in Fig.12.(b).

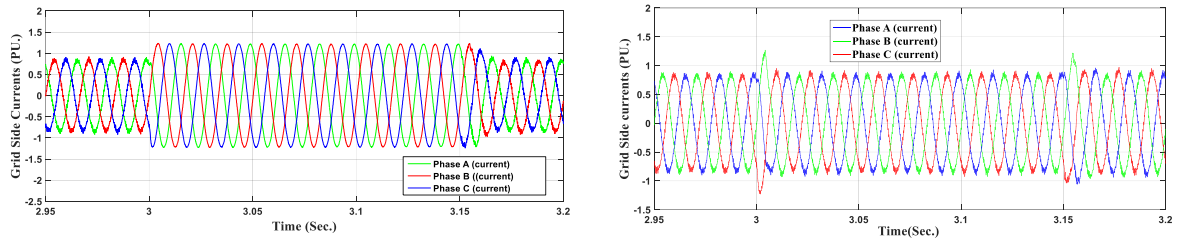

(a) (b)

Fig. 11. The grid side converter current (a) Without crowbar protection, (b) With crowbar protection.

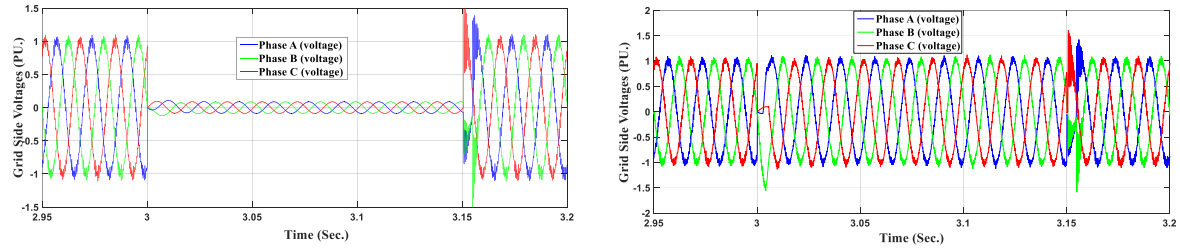

(a) (b)

Fig. 12. the grid side converter voltage (a) Without crowbar protection, (b) With crowbar protection.

The stator current and voltage are affected when the grid fault occurs. Therefore, the stator current during the fault and without using the crowbar protection system it found that the current value increase as shown in Fig.13.(a). In the other hand using crowbar protection system during the three-phase fault limiting the stator current to its rated value as shown in Fig.13. (b).

Fig.14. (a). shows that he stator voltage increased during the fault occurrence duration. Without the using of the crowbar protection system While in the case of using the crowbar protection the stator voltage value drops to its rated value as shown in Fig.14.(b).

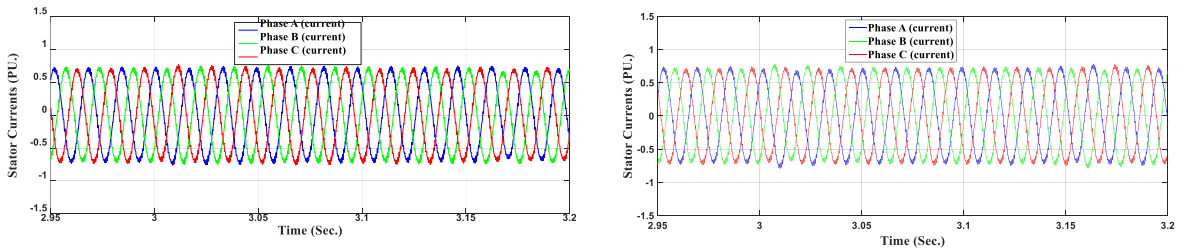

(a) (b)

Fig. 13. the stator current (a) Without crowbar protection, (b) With crowbar protection

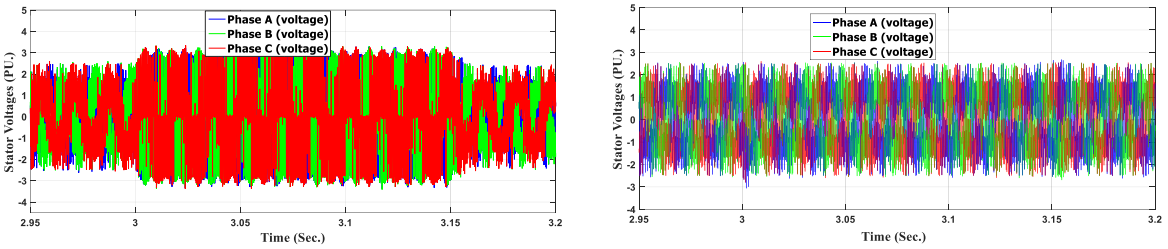

Fig. 14. stator voltage (a) Without crowbar protection, (b) With crowbar protection.

6. CONCLUSION

In this paper the performance of the WECS based PMSG has been studied with and without optimal inclusion of crowbar protection. The performance was investigated under three phase to ground fault for 150 m sec without using the crowbar protection. Then, the optimal crowbar resistors have been included optimal by application of an efficient optimizer call LAPO to protect the WECS based PMSG system. The obtained results verified that the performance the WECS based PMSG under fault was enhanced considerably with incorporating the crowbar optimally can decrease the stator currents to the allowable limits. Furthermore, DC voltage was reduced, and the reactive power was increased to its reference value compared with no existence of the protection system exist. As well as the active power profile was enhanced.

References

[1] Mousa, H.H.H., A.-R. Youssef, and E.E.M. Mohamed, Adaptive P&O MPPT algorithm based wind generation system using realistic wind fluctuations. International Journal of Electrical Power & Energy Systems, 2019. 112: p. 294-308.

[2] Abo-Khalil, A.G., H.H. El-Zohri, and K. Sayed, A 2 MW Wind Turbine Simulator for DFIG Wind Energy Generation Systems %J Sohag Engineering Journal. 2022. 2(1): p. 26-40.

[3] Qais, M.H., H.M. Hasanien, and S. Alghuwainem, Optimal Transient Search Algorithm-Based PI Controllers for Enhancing Low Voltage Ride-Through Ability of Grid-Linked PMSG-Based Wind Turbine. Electronics, 2020. 9(11).

[4] Mousa, H.H.H., A.-R. Youssef, and E.E.M. Mohamed, Hybrid and adaptive sectors P&O MPPT algorithm based wind generation system. Renewable Energy, 2020. 145: p. 1412-1429.

[5] Abo-Khalil, A.G. and K. Sayed, WIND TURBINE SIMULATION AND CONTROL USING SQUIRREL-CAGE INDUCTION GENERATOR FOR DFIG WIND ENERGY CONVERSION SYSTEMS %J Sohag Engineering Journal. 2021. 1(1): p. 1-15.

[6] Mahmoud, M.M., et al., Dynamic evaluation of optimization techniques–based proportional–integral controller for wind-driven permanent magnet synchronous generator. Wind Engineering, 2020. 45(3): p. 696-709.

[7] Nasiri, M., J. Milimonfared, and S.H. Fathi, A review of low-voltage ride-through enhancement methods for permanent magnet synchronous generator based wind turbines. Renewable and Sustainable Energy Reviews, 2015. 47: p. 399-415.

[8] Mousa, H.H.H., A.-R. Youssef, and E.E.M. Mohamed, Variable step size P&O MPPT algorithm for optimal power extraction of multi-phase PMSG based wind generation system. International Journal of Electrical Power & Energy Systems, 2019. 108: p. 218-231.

[9] Belkhier, Y., et al., Modified passivity-based current controller design of permanent magnet synchronous generator for wind conversion system. International Journal of Modelling and Simulation, 2020. 42(2): p. 192-202.

[10] 10. Liu, J., C. Zhao, and Z. Xie, Power and Current Limiting Control of Wind Turbines Based on PMSG Under Unbalanced Grid Voltage. IEEE Access, 2021. 9: p. 9873-9883.

[11] Oussama, M., A. Choucha, and L. Chaib, Fractional Order PI Controller Design for Control of Wind Energy Conversion System Using Bat Algorithm, in Renewable Energy for Smart and Sustainable Cities. 2019. p. 270-278.

[12] Soliman, M.A., et al., An Adaptive Fuzzy Logic Control Strategy for Performance Enhancement of a Grid-Connected PMSG-Based Wind Turbine. IEEE Transactions on Industrial Informatics, 2019. 15(6): p. 3163-3173.

[13] Okedu, K.E. and S.M. Muyeen, Enhanced performance of PMSG wind turbines during grid disturbance at different network strengths considering fault current limiter. International Transactions on Electrical Energy Systems, 2021. 31(8).

[14] Mahmoud, M.M., A.M. Hemeida, and A.-M.M. Abdel-Rahim. Behavior of PMSG wind turbines with active crowbar protection under faults. in 2019 innovations in power and advanced computing technologies (i-PACT). 2019. IEEE.

[15] Gencer, A., Analysis and Control of Fault Ride Through Capability Improvement PMSG Based on WECS Using Active Crowbar System During Different Fault Conditions. Elektronika ir Elektrotechnika, 2018. 24(2).

[16] Noureldeen, O., I.J.P. Hamdan, and C.o.M.P. Systems, A novel controllable crowbar based on fault type protection technique for DFIG wind energy conversion system using adaptive neuro-fuzzy inference system. 2018. 3(1): p. 1-12.

[17] Peng, L., B. Francois, and Y. Li. Improved crowbar control strategy of DFIG based wind turbines for grid fault ride-through. in 2009 twenty-fourth annual IEEE applied power electronics conference and exposition. 2009. IEEE.

[18] Hamdan, I. and O. Noureldeen, An Overview of Control Method with Various Crowbar Techniques of Wind Turbines during Power System Faults. SVU-International Journal of Engineering Sciences and Applications, 2021. 2(1): p. 35-45.

[19] Qais, M.H., H.M. Hasanien, and S. Alghuwainem, A novel LMSRE-based adaptive PI control scheme for grid-integrated PMSG-based variable-speed wind turbine. International Journal of Electrical Power & Energy Systems, 2021. 125.

[20] Okedu, K.E. and H. Barghash, Enhancing the Transient State Performance of Permanent Magnet Synchronous Generator Based Variable Speed Wind Turbines Using Power Converters Excitation Parameters. Frontiers in Energy Research, 2021. 9.

[21] Nasiri, M., A. Arzani, and M. Savaghebi, Current limitation for the machine side converter of permanent magnet synchronous generator wind turbines during grid faults. IET Renewable Power Generation, 2021. 14(17): p. 3448-3456.

[22] Wang, D., C. Liu, and G. Li, An Optimal Integrated Control Scheme for Permanent Magnet Synchronous Generator-Based Wind Turbines under Asymmetrical Grid Fault Conditions. Energies, 2016. 9(4).

[23] Noureldeen, O. and I. Hamdan, Design and Analysis of Combined Chopper-Crowbar Protection Scheme for Wind Power System Based on Artificial Intelligence, in 2018 Twentieth International Middle East Power Systems Conference (MEPCON). 2018. p. 809-814.

[24] Nematollahi, A.F., A. Rahiminejad, and B.J.A.S.C. Vahidi, A novel physical based meta-heuristic optimization method known as lightning attachment procedure optimization. 2017. 59: p. 596-621.

[25] Nematollahi, A.F., A. Rahiminejad, and B.J.A.S.C. Vahidi, A novel multi-objective optimization algorithm based on Lightning Attachment Procedure Optimization algorithm. 2019. 75: p. 404-427.

[26] Taher, M.A., et al., Optimal power flow solution incorporating a simplified UPFC model using lightning attachment procedure optimization. 2020. 30(1): p. e12170.

[27] Youssef, H., S. Kamel, and M. Ebeed. Optimal power flow considering loading margin stability using lightning attachment optimization technique. in 2018 Twentieth international middle east power systems conference (MEPCON). 2018. IEEE.

[28] Hashemian, P., A.F. Nematollahi, and B.J.A.i.e.r. Vahidi, A novel approach for optimal DG allocation in distribution network for minimizing voltage sag. 2019. 6(1): p. 55-73.

[29] Ebeed, M., et al., An Improved Lightning Attachment Procedure Optimizer for Optimal Reactive Power Dispatch With Uncertainty in Renewable Energy Resources. IEEE Access, 2020. 8: p. 168721-168731.

[30] Khan, N.H., et al., A Novel Modified Lightning Attachment Procedure Optimization Technique for Optimal Allocation of the FACTS Devices in Power Systems. IEEE Access, 2021. 9: p. 47976-47997.

[31] Saleh, B., et al., Design of PID Controller with Grid Connected Hybrid Renewable Energy System Using Optimization Algorithms. Journal of Electrical Engineering & Technology, 2021. 16(6): p. 3219-3233.

APPENDIX

A.1 Specification of wind turbine

The coefficients C1 to C6	C_1= 0:5176	C_4=5
	C_2=116	C_5= 21
	C_3=0:4	C_6=0:0068
Blade radius	R_b = 35:25 m	
Air density	ρ_{air} = 1:225 kg/m3	
Optimal tip speed ratio	λ_{max} = 8.1	
Maximum Power Coefficient	$C_{p\,max}$ = 0.48	

Appendix 2. Five-phase PMSG parameters

Rated power	P =1:5 MW
Pole pairs number	n_p =40
Stator resistance	R_s = 3:17 m ohm
Stator inductance	L_s = 3:07 mH
Moment of inertia	J =10000 kg/m2
Flux linkage	ψ= 7:0172 wb

Appendix 3. DC bus and gird parameters

Dc-link voltage	Vdc =1150V
Capacitor of the dc-link	C =0:023 F
Grid voltage	V_q =575 V
Grid frequency	F =60 Hz
Grid resistance	R_q =0:003 pu
Grid inductance	L_q =0:3 pu